Transformation of surface water and groundwater and water balance in the agricultural irrigation area of the Manas River Basin, China

Yang Guang[1,2], He Xinlin[1,2*], Li Xiaolong[1,2], Long Aihua[1,3], Xue Lianqing[1]

(1. *College of Water & Architectural Engineering, Shihezi University, Shihezi 832003, China*;
2. *Xinjiang Production & Construction Group, Key Laboratory of Modern Water-Saving Irrigation, Shihezi 832003, Xinjiang, China*;
3. *China Institute of Water Resources and Hydropower Research, Beijing 100038, China*)

Abstract: Calculation of the water balance is very important to relieve the pressure on water resources in arid agricultural irrigation areas. This research focused on irrigation water balance calculations in the Manas River Basin of the southern margin of the Junggar Basin of China, and aimed to analyze the groundwater level dynamic trend and response characteristics of the basin water cycle under water-saving irrigation measures. The surface water and groundwater coupling model of MIKE 11-Visual MODFLOW was used to simulate rainfall runoff in mountainous areas, and quantify the contribution of water balance components in the plain irrigation area. Convergence of the delayed watershed in the mountain area was obvious, and when the river runoff exceeded 200 m^3/s, the error in the runoff simulation was large. The water balance in the plain agricultural irrigation area was in a negative equilibrium state, and the difference between recharge and discharge was −2.65 billion m^3. The evapotranspiration was 24.49 billion m^3 under drip irrigation, accounting for only approximately 51% of the total discharge. The lateral discharge of the unsaturated and saturated aquifers was 15.38 billion m^3, accounting for approximately 32% of the total discharge. The main reason for the groundwater decline in the irrigation area was closely related to the extraction of groundwater, because the amount of recharge and discharge in the natural state was approximately identical. The MIKE 11-Visual MODFLOW model produced accurate results, and the research method provided a new exploration technique to quantify the effect of water supply mode on the groundwater table. The model is suitable for the management of water resources in arid areas.

Keywords: water balance, coupling model, surface water and groundwater, water saving irrigation, Manas River Basin
DOI: 10.25165/j.ijabe.20171004.3461

Citation: Yang G, He X L, Li X L, Long A H, Xue L Q. Transformation of surface water and groundwater and water balance in the agricultural irrigation area of the Manas River Basin, China. Int J Agric & Biol Eng, 2017; 10(4): 107–118.

1 Introduction

The arid desert oasis area in China accounts for only 4%-5% of the arid area; however, because more than 90% of the population in the arid area and more than 95% of the social wealth are concentrated in the oasis area, it is very important for the development of social economy[1]. In recent years, the rapid development of large areas of farmland irrigation, industry, agriculture and urbanization has led to an increasing demand for water resources. Therefore, it is necessary to integrate the management of surface water and groundwater resources to realize the

Received dare: 2017-04-30 **Accepted data:** 2017-07-02
Biographies: Yang Guang, PhD student, Associate Professor, research interests: Hydrology and water resources, Email: mikeyork@163.com; **Li Xiaolong**, Master, Associate Professor, research interests: Hydrology and water resources, Email: 13150401816@163.com; **Long Aihua**, PhD, Professor, research interests: Hydrology and water resources, Email: ahlong@ iwhr.com; **Xue Lianqing**, PhD, Professor, research interests: Hydrology and water resources, Email: lqxue@hhu.edu.cn;
***Corresponding author: He Xinlin,** PhD, Professor, research interests: Hydrology and water resources. Key Laboratory of Modern Water-Saving Irrigation of Xinjiang Production & Construction Corps, Shihezi University, Shihezi 832003, China. Tel: +86-15309934677, Email: hexinlin2002@163.com.

sustainable utilization of water resources[2]. Joint simulation of surface water and groundwater is a powerful tool to achieve this goal[3]. In the endorheic Okavango River system in southern Africa, a balance between human and environmental water demands was needed. Based on the groundwater simulation software MODFLOW-96 a large-scale (1 km^2 grid) coupled surface water-groundwater model was developed to study the impacts of upstream and local interventions[4]. The model is composed of a surface water flow component based on the diffusive wave approximation of the Saint-Venant Equations, a groundwater component, and a relatively simple vadose zone component for calculating the net water exchange between land and atmosphere[5]. The temporally variable impact of groundwater-surface water interactions further highlights the necessity to consider seasonal effects when assessing the significance of floodplain processes and functions[6]. The fully distributed physically based model MIKE SHE was used to simulate the individual hydrological components of the total water balance for the Paya Indah Wetlands watershed in the west of Peninsular Malaysia. And results revealed that the overall water balance was predominantly controlled by climate variables. Application of the model to the watershed provided detailed estimates of the total water balance for a first-order catchment in which actual evapotranspiration represented approximately 65% and 58% during the calibration and validation periods, respectively, while overland flow represented 12.38% and 12.3% of the total rainfall[7]. The difference between the inflow and outflow of the watershed lake system was taken as surface storage. Overall, the model gave a reasonable output with a total error of less than 1% of the total rainfall, which in turn indicated that the interaction among hydrologic components was satisfactorily sustained[8]. Patterns of groundwater-surface water interaction were explored throughout the watershed during 1970-2003 using a coupled SWAT-MODFLOW model tested against streamflow, groundwater level, and field-estimated reach-specific groundwater discharge rates. And results showed that the average annual groundwater discharge was 20.5 m^3/s, with maximum and minimum rates occurring in September-October and March-April, respectively. Annual average rates increased by approximately 0.02 m^3/s over the 34-year study period[9]. These changes were negligible compared to the average annual discharge rate, although 70% of the stream network experienced an increase in groundwater discharge rate during the study period[10]. Results such as these can assist with water management, identifying potential locations of heavy nutrient mass loading from the aquifer to streams, and ecological assessment and planning focused on locations of high groundwater discharge[11].

The Manas River Basin is typical of the mountain oasis desert systems that are found in arid regions of China, and in which the surface typography, boundary conditions and the system of agricultural water use are very complicated[12]. The Manas River irrigation area is an important part of the basin and water management here is crucial to sustainable development. The objective of this study was to develop strategies for the rational management and sustainable utilization of water resources in the Manas River irrigation area[13]. According to the dynamics of river and groundwater dynamics theory, we applied the MIKE 11-Visual MODFLOW surface water and groundwater coupling model to simulate rainfall runoff in the mountainous area in of this basin, and to quantify the contribution of water balance components in the plain irrigation area. Detailed calculation of contributions from irrigation water cycle components, and analysis of dynamic changes of groundwater level responses to the water cycle under water saving irrigation methods, revealed the transformation relationship between surface water and groundwater in this important irrigation area.

2 Materials and methods

The Manas River Basin is located in the north of the Tianshan Mountains, in the southern margin of the Junggar Basin, and includes Shihezi City, Manasi County, and Shawan County. Located at 43°27'-45°21'N, 85°01'-86°32'E, the basin has an area of 3.41×10^4 km^2 (Figure 1). The basin has a typical temperate continental climate. The annual rainfall is approximately 700-

1000 mm in the southern alpine area, 300-400 mm in the low mountain and hilly area, and approximately 200 mm in the central plain area. The mountain area has glacier snow that persists throughout the year, but the plain area has an annual average temperature of 6°C and a frost-free period of 160-170 d. Annual sunshine is 2750-2840 h, and the duration of temperatures that exceed 10°C is 3250-3900 h. Annual total radiation is in the range 126-135 kcal/cm^2. In the southern piedmont alluvial fan, the phreatic water saturated zone has a thickness of more than 400 m, and the water table and water quality are stable in the single structure of the phreatic water storage area. The aquitard of the groundwater aquifer is incomplete in the middle plain area, and the upper shallow phreatic aquifers from south to north gradually become thinner and form a perched aquifer. The lower system is comprised of multi-layer confined water and is an artesian aquifer (Figure 2).

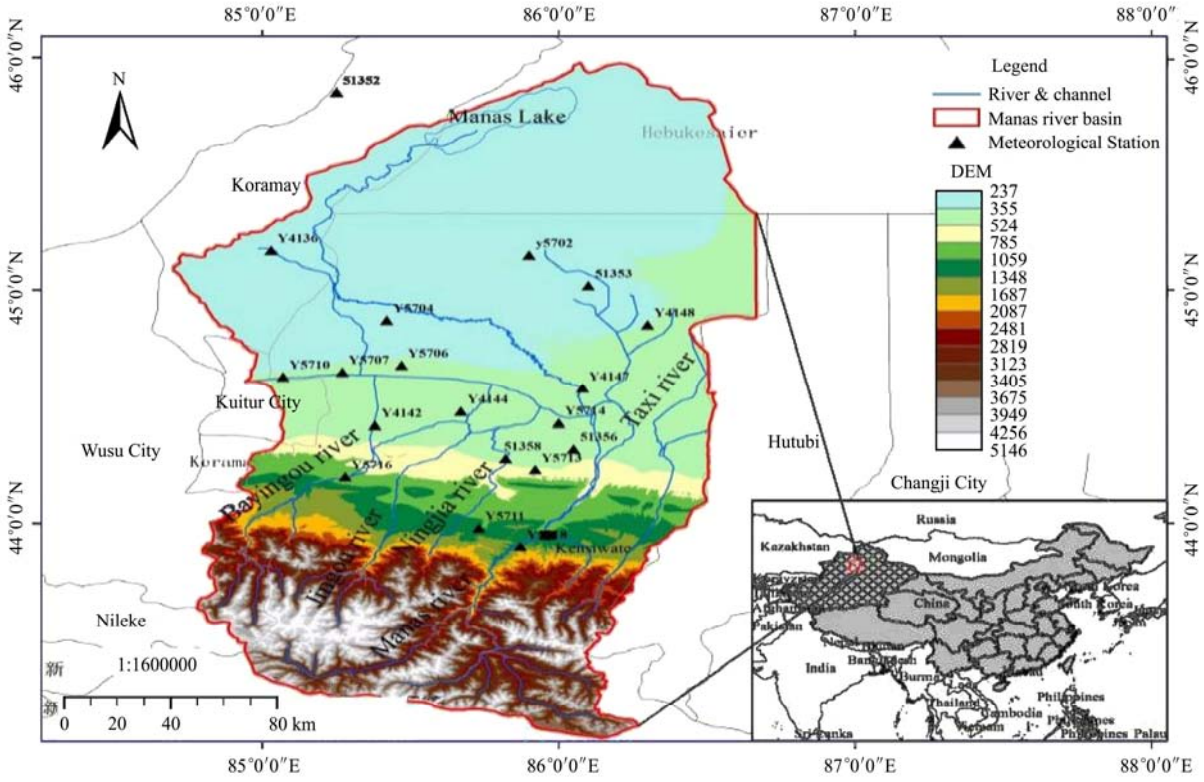

Figure 1 Location of study area and distribution river network

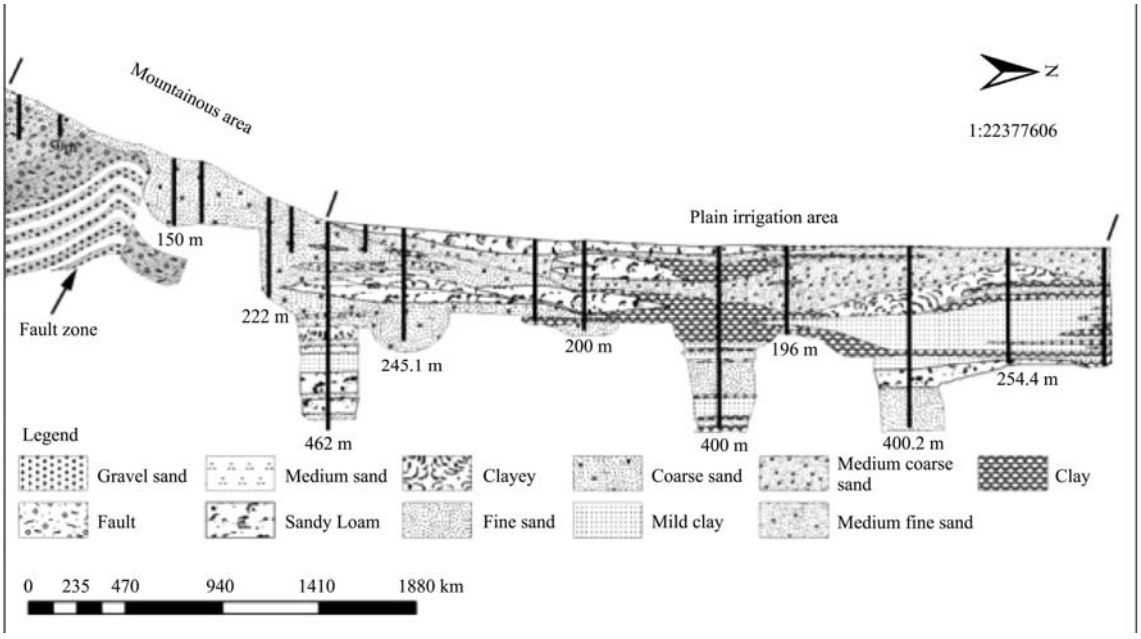

Figure 2 Hydrogeological profile of the study area

The process of water utilization in the Manas River Plain is mainly conducted using a combined "collection-diversion-utilization-drainage" system. In addition to using natural precipitation, the Manas River irrigation area mainly distributes water from the Manas River through channels and uses wells to exploit groundwater. Thus, this part of the water cycle is transformed under the influence of both natural factors and irrigation activities. Therefore, from the perspective of the development and utilization of water resources, the water cycle of the combined network of canals and wells is mainly reflected in the transformation between surface water and groundwater, and is affected by external environmental changes. Through water recharge, both runoff and discharge can affect the groundwater circulation, thus affecting the water balance of the irrigation area[14].

Data for the surface water and groundwater coupling model included meteorological data and runoff data for the period Jan 1, 2005 to Dec 31, 2015, watershed parameters and initial conditions, the river shape, hydraulic structure, hydrology station location, riverbed cross-section, hydrological data at the boundary of the model, elevation data, groundwater depth, groundwater exploitation data, soil type and land use. The study used meteorological data from the Mosuowan research station in Shihezi, from Paotai, Mosuowan, Shihezi and Wulanwusu counties, and from 15 regional meteorological stations.

2.1 One dimensional hydrodynamic MIKE11 model

The MIKE11/HD model can visually simulate the flow of river water. The model is suitable for hydraulic calculations of upland (mountain) and lowland (plain) rivers, including physical configurations of a single channel river, forked river and river ring. The model has many advantages, such as a reliable algorithm, stable calculation, convenient processing, and powerful hydraulic structure adjustment. The MIKE11/HD model uses the material flow equation and momentum conservation equation based on integral vertical one-dimensional constant flow Saint Venant Equations to simulate the flow of rivers and the water dynamic state[15].

$$\frac{\partial A}{\partial t}+\frac{\partial Q}{\partial x}=q \tag{1}$$

$$\frac{\partial Q}{\partial t}+\frac{\partial}{\partial x}\left(\frac{\alpha Q^2}{A}\right)+Ag\frac{\partial h}{\partial x}+\frac{gQ|Q|}{c^2AR}=0 \tag{2}$$

where, A is the cross section area, m^2; Q is flow discharge, m^3/s; x and t are the coordinates of point space and time, respectively; h is the water level, m; q is the lateral flow, m^3/s; C is the Chezy coefficient; R is the hydraulic radius; α is a momentum correction factor; g is the acceleration of gravity, m/s^2.

The MIKE11/NAM rainfall runoff model can be used independently, but can also be coupled with the MIKE11/HD hydrodynamic model to calculate the single or multiple runoff-producing area in a basin. When coupled with the MIKE11/HD model, the rainfall runoff is used as a coupling calculation to determine inflow into the MIKE11/HD hydrodynamic model. The Nash-Sutcliffe model efficiency coefficient (E_{ns}) and decision coefficient (R^2), as defined by the following equations, were used to evaluate the performance of the model[16].

$$E_{ns}=1-\frac{\sum_{i=1}^{n}(Q_{obs,i}-Q_{sim,i})^2}{\sum_{i=1}^{n}(Q_{obs,i}-\bar{Q}_{obs})^2} \tag{3}$$

$$R^2=\frac{[\sum_{i=1}^{n}(Q_{obs,i}-\bar{Q}_{obs})(Q_{sim,i}-\bar{Q}_{sim})]^2}{\sum_{i=1}^{n}(Q_{obs,i}-\bar{Q}_{obs})^2\sum_{i=1}^{n}(Q_{sim,i}-\bar{Q}_{sim})^2} \tag{4}$$

where, $Q_{obs,i}$ is the observed flow value for time step i, m^3/s; $Q_{sim,i}$ is the simulated flow value of time step i, m^3/s; n is the total number of steps, d; $\bar{Q}_{obs}$ is the average value of the observed flow during the simulation period, m^3/s; $\bar{Q}_{sim}$ is the average value of the simulated flow during the simulation period, m^3/s.

2.2 Three-dimensional groundwater numerical model Visual MODFLOW and the water balance equation

Visual MODFLOW is the most complete and easy-to-use simulation software for three-dimensional groundwater flow and contaminant transport simulation[17]. In Visual MODFLOW, the model grid, the input parameters and the results can be visualized in the form of a section and plan for the study area. Based on a study of aquifer structure, groundwater recharge and discharge conditions, and groundwater system characteristics, we established a heterogeneous isotropic three-dimensional unsteady flow mathematical model as

described by the following equations:

$$\frac{\partial}{\partial x}\left(k\frac{\partial H}{\partial x}\right)+\frac{\partial}{\partial y}\left(k\frac{\partial H}{\partial y}\right)+\frac{\partial}{\partial z}\left(k\frac{\partial H}{\partial z}\right)+W=\mu\frac{\partial H}{\partial t}$$
$$(x,y,z)\in D \quad (5)$$
$$H|_{B1}=H_1(x,y,z,t)\quad (x,y,z)\in B1,\ t>0$$
$$k\frac{\partial H}{\partial n}\bigg|_{B2}=q(x,y,z,t)\quad (x,y,z)\in B2,\ t>0$$

where, μ is the Specific yield; D is the seepage zone, m; K is the aquifer hydraulic conductivity, m/d; H is the groundwater head, m; W is the volumetric flux per unit value representing sources and sinks of water (such that W<0.0 for outflow from the groundwater system, and W>0.0 for inflow), m/d; S_s is the aquifer specific yield; H_0 (x, y, z) is the initial flow field head, m; t is time, d; n is the direction of the second boundary outward normal; H_1 (x, y, z, t) is the head distribution value of the first boundary, m; $B1$ is the first class boundary; q (x, y, z, t) is the discharge per unit width of the second boundary, m^3/d; and $B2$ is the second boundary.

The number of water cycles is expressed in a given time scale space in which the motion of water is continuous, maintaining a balance in the quantity, and following the law of conservation of mass. According to the condition of water recharge and discharge in the Manas River irrigation area, the water balance equation can be established as follows:

$$P+I+Q_{in}-Q_{out}-E-W\pm D_{UZ}\pm D_{SZ}=0 \quad (6)$$

where, P is the precipitation infiltration recharge; I is the irrigation water recharge; Q_{in} is the groundwater lateral aquifer inflow; Q_{out} is the groundwater lateral aquifer outflow; E is irrigation evapotranspiration; W is the artificial exploitation; D_{uz} is the change of water storage in the unsaturated aquifer; and D_{sz} is the change of water storage in the saturated aquifer.

3 Results and discussion

3.1 MIKE11 model calibration and validation

Both the hydrodynamic module and rainfall runoff module are included in the MIKE 11 model. We applied the coupled one-dimensional hydrodynamic and rainfall runoff model to a section of the Manas River Basin upstream of the Kensiwate hydrological station (Figure 1). We optimized the space-time distribution data of water supply quantity of surface water and groundwater exploitation as the source-sink model of groundwater input to achieve data exchange. Snowmelt and the rainfall runoff processes in a mountainous area were simulated using the rainfall runoff model.

The mountain runoff becomes lateral inflow to the hydrodynamic model for the river network. According to the dynamic changes of water resources in the basin and aquifer structure, a groundwater heterogeneous isotropic three-dimensional unsteady flow mathematical model was established using Visual MODFLOW. Furthermore, the finite difference method was used to discretize the model. The dynamic simulation of the whole groundwater system was realized by the dynamic simulation of the boundary condition and the vertical water exchange quantity, and the fitting of the dynamic flow field of the phreatic aquifer and the confined aquifer.

The hydraulic conditions of the upstream region of the Manas River network are simple, and there is no influence on flow pattern by any large-scale river water control projects. The upper boundary of the model was defined by daily water flow data at Hongshanzui for the period Jan 1, 2005 to Dec 31, 2015, while the lower boundary was defined by daily water level data at the Kensiwate hydrological station for the same period.

The calibration of the model is automatically determined by the MIKE11/NAM model. The main parameter of the hydrodynamic model is the riverbed roughness. Based on the riverbed roughness change, until Kensiwate hydrological station flow simulation and measured values to achieve better fitting results. The period from Jan 1, 2005 to Dec 31, 2009 was used for model calibration, and the period from Jan 1, 2010 to Dec 31, 2015 was used for model validation. Figure 3 compares the simulated runoff to measured runoff for the Kensiwate hydrological station in the calibration and validation periods. The calibrated parameter values for the study area are shown in Table 1.

The results showed that the dynamic simulation of the rainfall runoff at the station was quite satisfactory. The hydrodynamic model simulated an unstable flow channel using the Abbott-Ionescu six-point implicit finite

difference scheme in which the discrete linear equations are solved by a "double sweep" method. After calibration, the simulated runoff was in good agreement with the actual runoff (Table 2). In addition, actual precipitation and simulated runoff showed a consistent correspondence. However, the comparison of calculated and observed runoff shows that the simulation of small values of runoff was better than the simulation of larger values (Figure 3). In addition, the simulated maximum runoff was always less than the observed maximum runoff, a result that was directly related to the model parameter setting.

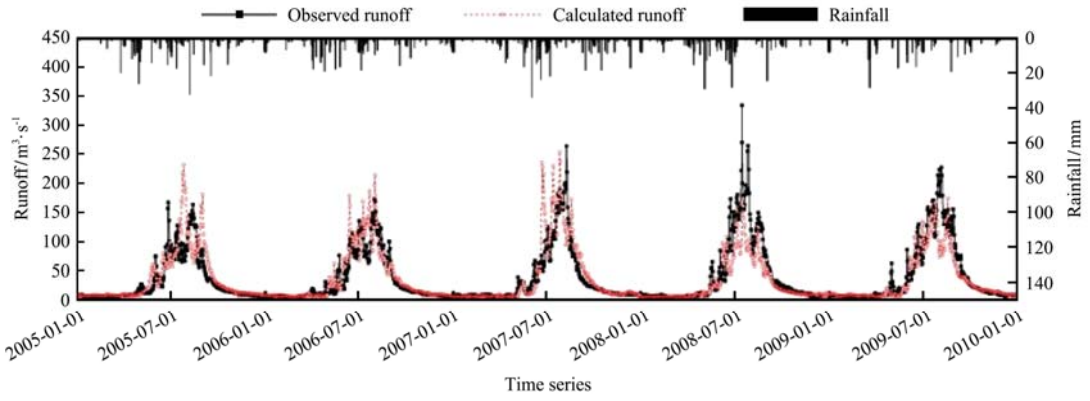

a. Model calibration

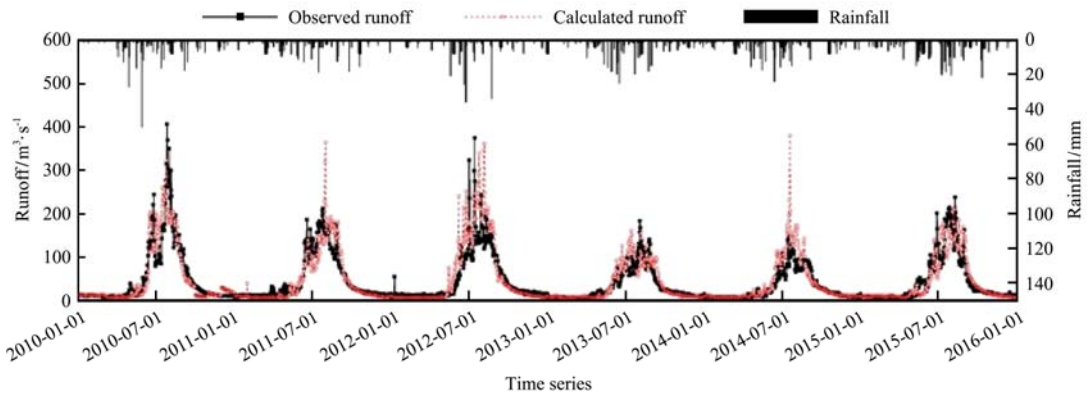

b. Model verification

Figure 3 Observed and simulated runoff at the Kensiwate hydrological station during

Table 1 Calibrated model parameters

Parameter	Parameter meaning	General range of values	Initial value	Calibrated value
U_{max}	Maximum water content of surface reservoir/mm	10-25	15	15.111
L_{max}	Maximum water content in soil layer and root zone/mm	50-250	150	180.541
C_{QOF}	Overland flow coefficient	0-1	0.6	0.601
CK_{IF}	Interflow constant/h	500-1000	1000	710.250
TOF	Critical value of overland flow	0-1	0	0.941
TIF	Critical value of interflow	0-1	0	0.825
TG	Critical value of groundwater recharge	0-1	0	0.801
CK_{12}	Overland flow and interflow time constant/h	3-48	10	31.464
CK_{BF}	Base flow time constant/h	500-5000	2000	2615.331
n-Manning	River roughness	0.02-0.04	0.03	0.035

Table 2 Simulation results evaluation

Category	Discharge point	Coefficient		Regression parameters	
		E_{ns}	R^2	Slope	Intercept
Calibration	Kensiwate	0.69	0.66	0.75	7.89
Validation	Kensiwate	0.76	0.85	0.96	4.45

The linear regressions of observed and simulated runoff at the Kensiwate hydrological station during model calibration and verification (Figure 4) show that the correlation between observed and simulated runoff was good, and most of the data points were located in the 95%

confidence interval. However, the error in simulated runoff increased as the magnitude of runoff increased. During validation the correlation coefficient was 0.8543, which indicated a better simulation precision than during calibration, as expected. The Nash-Sutcliffe coefficients were 0.69 and 0.76 in the model calibration and validation periods, respectively.

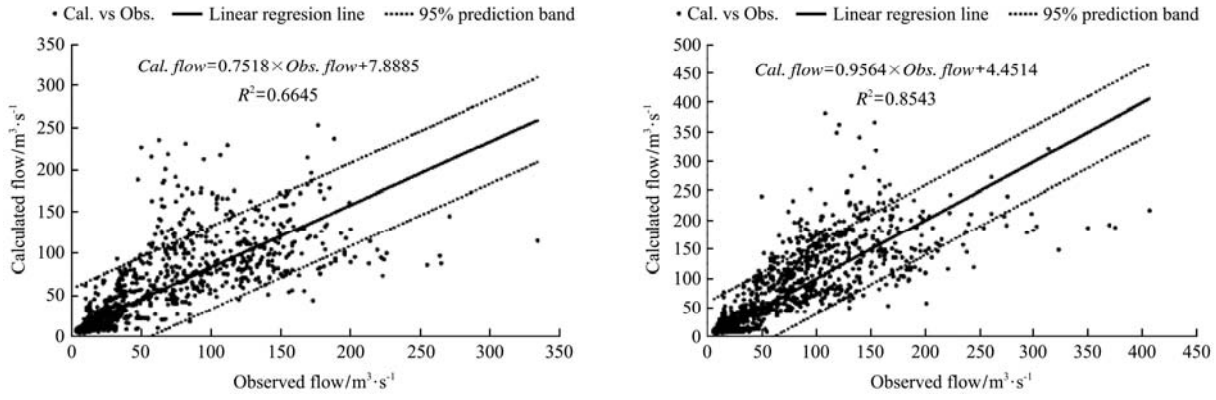

a. Model calibration b. Model verification

Figure 4 Linear fitting of observed and simulated runoff at the Kensiwate hydrological station during

3.2 Visual MODFLOW groundwater model calibration and results

Visual MODFLOW was used to establish a heterogeneous isotropic three-dimensional unsteady flow mathematical model of groundwater, and the finite difference method was used to discretize the study area. The horizontal direction of the study area was divided into 400 rows and 410 columns of 360 m × 560 m grid cells, such that each grid area was approximately 0.2 km^2. The Xiayedi irrigation area, Mosuowan irrigation area, Shihezi irrigation area, Anjihai irrigation area and Jingouhe irrigation area were set as "active cells" and the remaining area was set as "non-active cells". Non-active cells were excluded from the calculation process in the model. The groundwater aquifer generally was divided into 10 vertical aquifer layers, each with a thickness of 300 m. The model simulation period was Jan 1, 2013 to Dec 31, 2013, a total of 365 d. The water level values of observation flow and simulated flow in Dec 31, 2013 were compared and analyzed, and the accuracy of the model was analyzed with the error of both.

The surface water recharge of groundwater as calculated using MIKE11, as well as simulated rainfall recharge, canal seepage and irrigation return water supply are shown in Table 3.

Table 3 Statistics of simulated groundwater recharge

Irrigation area name	Agricultural farms	Groundwater/×10^4 m^3	Surface water/×10^4 m^3	Precipitation/mm	Control area/×10^8 m^2	Recharge depth/mm·a^{-1}
Shihezi	Shihezi head farm	10 230.00	10 569	197.9	3.6	905.34
	Shihezi township	293.00	4165			
Xiayedi	121st	3331.8	6418	127.8	7.3	680.63
	122nd	305.94	4993			
	132nd	1193.4	5425			
	133rd	233.46	4396			
	134th	238.68	4219			
	135th	1847.88	3049			
	136th	2148.12	2618			
Mosuowan	147th	3925.00	5004	132.7	5.8	852.90
	148th	2862.00	7912			
	149th	3443.00	6073			
	150th	5587.00	6894			
Jingouhe & Anjihai	144th	1977.00	6364	211.0	1.9	1701.87
	143rd	5050.00	15 096			
	141st	624.00	4283	122.8	4.1	634.48
	142nd	9530.00	6751			

The model simulations showed that the southern part of the phreatic aquifer in the study area mainly received mountain front lateral recharge, canal seepage, and rainfall infiltration. In contrast, the northern confined aquifer mainly received the southern aquifer system lateral recharge, canal seepage, irrigation return water and precipitation infiltration. The excretion was mainly agricultural irrigation, evaporation, transpiration and lateral discharge to the northern border. Based on the above analysis, the boundary conditions in the study area (Figure 5) conformed to the following generalization: the southern boundary of the study area was the lateral recharge boundary; the northern boundary was the lateral drainage boundary, and can be generalized into secondary types of flow boundaries. The east and west boundaries between the outer sector and the adjacent watershed (where there was no large-scale exploitation of groundwater) were characterized as secondary boundary types of either impermeable boundary or zero flow boundary. In the model, we selected the wall boundary.

The observed groundwater data in the study area were provided by the local water conservancy department. An integrated ZKGD-3000 water level and water temperature instrument was used widely to monitor the groundwater, and the depth of the probe was located 8-215 m below the water table. After rejecting abnormal values of groundwater observation data, the remaining data from 43 representative observation wells (Figure 5) were used for the groundwater numerical simulation. Pumping wells represented groundwater sinks in the model. The depth of the open bedrock zones in the wells ranged from 80 m to 250 m below the ground surface. Those zones were assigned as the pumping interval in the model. The pumping rates of the wells were distributed over the length of the open-hole interval of the pumping wells, which intersected multiple model layers. The large number of pumping wells within the study area presented great difficulties in simulating the pumping, so we conceptualized a number of small pumping wells as a large pumping well.

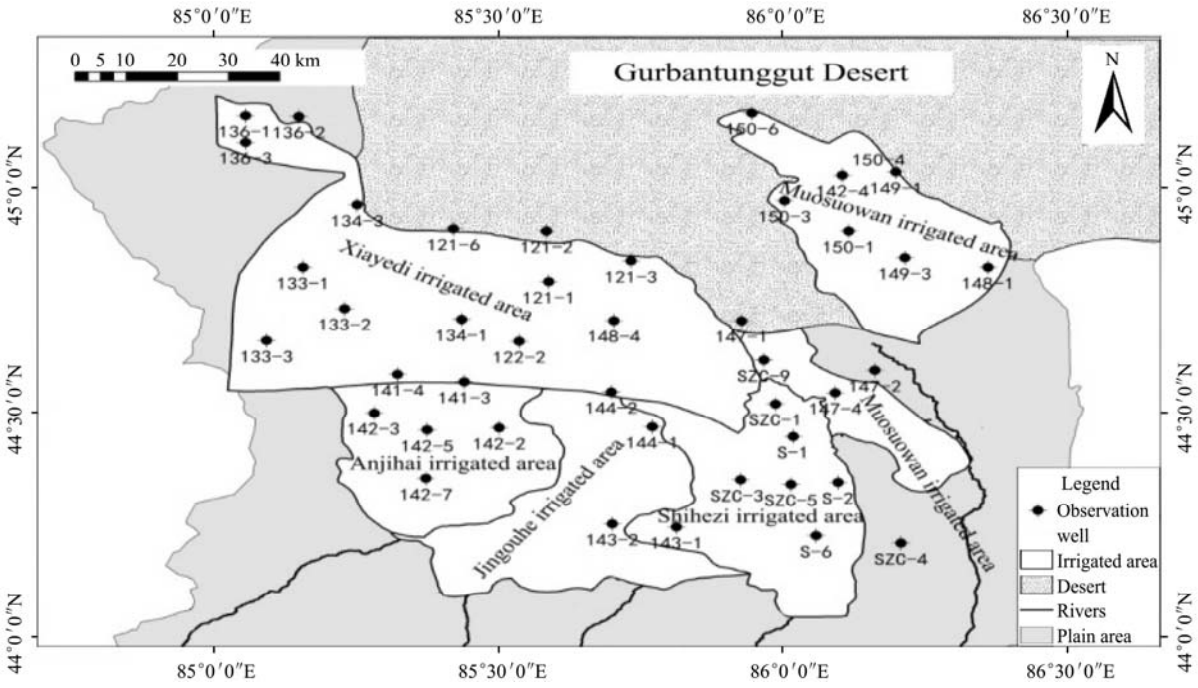

Figure 5 Distribution of Manas River irrigation area and groundwater observation well locations

The main parameters of the model are hydraulic conductivity, specific yield and specific storage[18]. The groundwater flow model calibration procedure involves adjusting model parameters so that the simulated results provide an acceptable match to the observed conditions while maintaining reasonable parameter values. Through a combination of automatic model parameter identifications and manual parameter adjustments, we analyzed the fit between the actual and simulated groundwater flow fields, taking the groundwater levels of the 43 long-term observation wells as the basis for parameter calibration. The calculated results for the

water balance were used as the standard for model parameter verification. Table 4 shows the hydrological parameters for each type of soil after the model calibration.

The model used the WHS solver in Visual MODFLOW, which uses the conjugate gradient stability (Bi-CGSTAB) acceleration program. After a series of model simulations, the optimization of parameters and the optimization of wells, a set of simulation results were obtained for calculating the groundwater level and the goodness of fit of monitoring wells (Figure 6).

Table 4 Calibrated hydrogeological parameters for different soil types

Soil types	Conductivity /m·s^{-1}	Specific yield (Sy)	Specific storage /m^{-1}
Sandy gravel	8.68E-04	0.10	1.00E-05
Middle sand	4.05E-04	0.06	1.00E-05
Clay	5.79E-07	0.30	1.00E-05
Medium coarse sand	5.21E-04	0.15	1.00E-05
Mild clay	2.31E-06	0.30	1.00E-05
Medium fine sand	3.47E-04	0.12	1.00E-05
Fine sand	2.31E-04	0.11	1.00E-05
Conglomerate	8.68E-04	0.10	1.00E-05
Fine silty sand	5.79E-04	0.07	1.00E-05

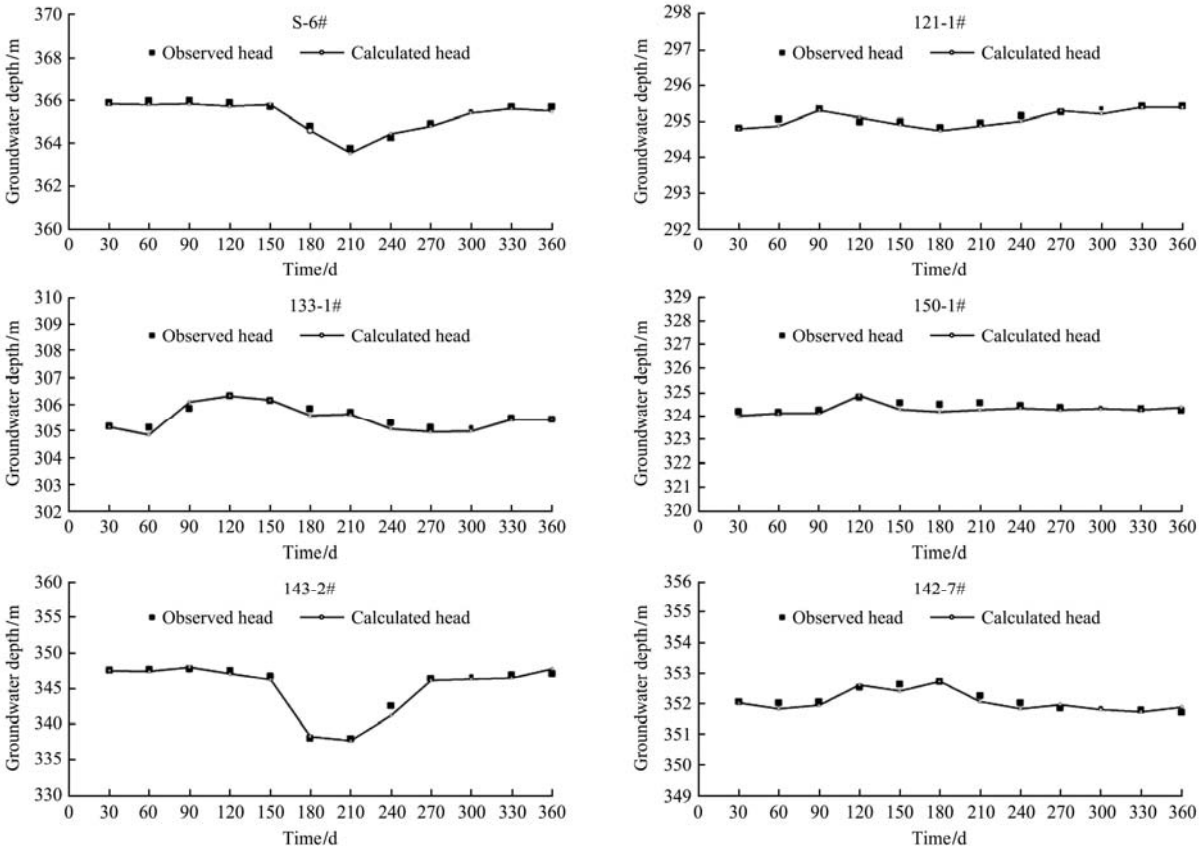

Figure 6 Observed and simulated groundwater levels for selected wells in the Manas River irrigation area

The dynamic change of groundwater level in the Manas River irrigation area was mainly caused by the change of water content in the aquifer, which was significantly affected by pumping wells. Because all pumping wells were shallow groundwater wells, groundwater level changes occurred mainly in the shallow aquifer. The simulation of the groundwater level dynamic change trend closely reflected the use of irrigation water for agricultural production. According to the agricultural production activities in different irrigation conditions in the Manas River irrigation area, we chose to display the observed and simulated groundwater levels in the Xiayedi irrigation area (wells 133-1# and 121-1#), the Muosuowan irrigation area (well 150-1#), the Anjihai irrigation area (well 142-7#), the Jingouhe irrigation area (well 143-2#) and the Shihezi irrigation area (well S-6#) (Figure 5).

For 5-9 months of the simulation time period, the groundwater levels of the Jinhegou and Shihezi irrigation areas experienced an obvious groundwater level decline of approximately 7 m, and the downward trend of groundwater levels was consistent with the irrigation period of cotton crop production in the area. The groundwater levels in the Anjihai, Mosuowan and

Xiayedi irrigation areas declined by approximately 2 m, but the drawdown amplitude was not obvious.

Figure 7 illustrates that the groundwater depth on Dec 31, 2013 in different locations of the irrigation area differed; this variation was due to differences in the pumping wells and the boundary conditions. In the Shihezi, Anjihai and Jingouhe irrigation areas groundwater was relatively deep and changes in groundwater level showed a slow decline. Furthermore, the effect of precipitation was not obvious, and the groundwater level did not rise even in the summer season when precipitation delivered a large amount of water. The annual 1-2 month irrigation groundwater depth decreases, because winter groundwater exploitation is low. The permeability of the aquifer was good in the Xiayedi and Mosuowan irrigation areas, and the soil texture was mainly composed of various kinds of sand, resulting in large pore sizes, good permeability, runoff and drainage. Due to the influence of the spring irrigation and the exploitation of groundwater, the groundwater depth decreased. After irrigation, the groundwater was recharged by the irrigation and the level rose gradually. Thus, there was a periodic fluctuation of groundwater depth according to the time of irrigation.

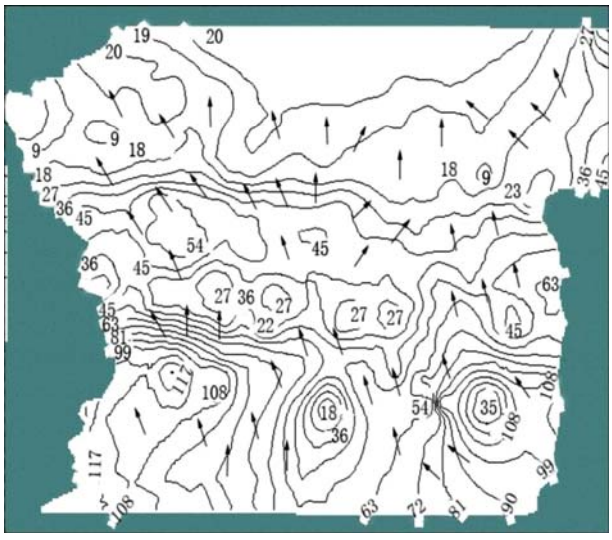

Figure 7 Groundwater flow field and direction in the Manas River irrigation area (Dec 31, 2013)

3.3 Water balance calculation in Manas River irrigation area

The Visual MODFLOW River package allows the user to introduce surface water boundary conditions into groundwater flow simulations[19]. The relationship between surface water and groundwater systems depends on the hydraulic gradient between surface water and groundwater. The result file from the MIKE11 model was imported into the Visual MODFLOW model to calculate the water balance of Manas River irrigation area.

The calculated water balance in Manas River irrigation area consisted of a total water recharge of approximately 45.31×10^8 m^3 and a boundary discharge water of approximately 47.96×10^8 m^3, a difference of approximately 2.65×10^8 m^3 that created a negative water balance (Table 5). The Manas River irrigation area surface input precipitation was 19.81×10^8 m^3 and accounted for 43.72% of the total water recharge. According to the MIKE11 simulation, the northern boundary of the study area contributed 12.8×10^8 m^3 of surface runoff, which accounted for 28.25% of the total water recharge. The inflow from the unsaturated aquifer was 10.24×10^8 m^3, and the inflow from the saturated aquifer was 2.46×10^8 m^3, accounting for 22.60% and 5.43% of the total water recharge, respectively. The main types of discharge were evapotranspiration, boundary discharge and groundwater extraction. The evaporation was 24.49×10^8 m^3, accounting for 51.06% of the total water discharge. Outflow surface runoff from the southern boundary of the study area was 2.81×10^8 m^3 and accounted for 5.86% of the total water discharge. The outflow from the unsaturated aquifer was 12.41×10^8 m^3, and the outflow from the saturated aquifer was 2.97×10^8 m^3; these accounted for 25.88% and 6.19% of the total water discharge, respectively.

Table 5 Summary of the water balance in the study area

	Component	Contribution /$\times10^8$ m^3	Total /$\times10^8$ m^3	Percentage of total/%
Recharge	Precipitation	19.81	45.31	43.72
	OL-north boundary inflow	12.8		28.25
	UZ-north boundary inflow	10.24		22.60
	SZ-north boundary inflow	2.46		5.43
Discharge	Evapotranspiration	-24.49	47.96	51.06
	OL-south boundary outflow	-2.81		5.86
	UZ-south boundary outflow	-12.41		25.88
	SZ-south boundary outflow	-2.97		6.19
	Groundwater pumping	-5.28		11.07
Water balance	Recharge-Discharge	-2.65		

Note: * OL-Overland flow; UZ-Unsaturated Zone; SZ-Saturated Zone.

4 Conclusions

In this research, the surface water and groundwater coupling model of MIKE 11-Visual MODFLOW was used to calculate the agricultural water use balance in Manas River irrigation area of China. The model simulations indicate the following conclusions:

1) There are obvious seasonal characteristics of runoff in the Manas River Basin, and the runoff increases as temperature increases. The rainfall runoff curve shows that the hysteresis is obvious in the mountainous area, and the corresponding relationship between the simulated runoff and the rainfall pattern is consistent. The model can well simulate runoff variations in different years, but the simulation results are better for small runoff values than for larger flows. When runoff exceeds 200 m^3/s, observed runoff is higher than the simulated runoff. The Nash-Sutcliffe coefficient for the model during the validation period model was 0.76, and the simulation results were acceptably accurate.

2) In the Manas River irrigation area, total water recharge is approximately 45.31×10^8 m^3, but boundary discharge is approximately 47.96×10^8 m^3, resulting in a net deficit of 2.65×10^8 m^3 and a negative water balance. Surface input precipitation is 19.81×10^8 m^3, accounting for 43.72% of the total water recharge. Surface runoff into the northern boundary of the study area is 12.8×10^8 m^3, accounting for 28.25% of the total water recharge. Evaporation amounting to 24.49×10^8 m^3 accounts for 51.06% of the total water discharge, and is the main type of discharge.

3) Three suggestions for managing water resources in the Manas River Basin are justified by the results of this study, as follows. Practices that increase the supply of surface water and reduce demand on groundwater can reduce groundwater depletion and increase sustainability. There is a limit to the efficiency of irrigation systems because of the potential for soil salinization; thus, where possible, irrigated crops should be converted to rainfed crops to reduce groundwater depletion. Furthermore, temporal disconnects between water supply and demand should be managed through conjunctive use of surface water and groundwater and the provision of increased water storage.

Acknowledgements

We acknowledge the support from the National Natural Science Fund (41601579, 41361096), National Key Development Program (2017YFC0404303, 2017YFC0404304, 2016YFC0501402), Excellent Youth Teachers Program of Xinjiang Production& Construction Corps (CZ027204).

[References]

[1] Wu C F, Déry S, Wu W C, Liu X B, Xiong J H, Gao W Q. A review of water resources utilization and protection in Southwest China. Sci Cold Arid Reg, 2015; 7: 736–746.

[2] Yang G Q, Guo P, Li R H, Li M. Optimal allocation model of surface water and groundwater based on queuing theory in irrigation district. Transactions of the CSAE, 2016; 32(6): 115–120. (in Chinese)

[3] Chung I M, Lee J, Kim N W, Na H, Chang S W, Kim Y C, et al. Estimating exploitable amount of groundwater abstraction using an integrated surface water-groundwater model: Mihocheon watershed, South Korea. Hydrological Sciences Journal, 2015; 60(5): 863–872.

[4] Bauer P, Gumbricht T, Kinzelbach W. A regional coupled surface water/groundwater model of the Okavango Delta, Botswana. Water Resources Research, 2006; 42(4): 1–15.

[5] Krause S, Bronstert A, Zehe E. Groundwater-surface water interactions in a North German lowland floodplain-implications for the river discharge dynamics and riparian water balance. Journal of hydrology, 2007; 347(3): 404–417.

[6] Basharat M, Hassan D, Bajkani A A. Surface water and groundwater nexus: Groundwater management options for indus basin irrigation system. International Waterlogging and Salinity Research Institute (IWASRI), Lahore, Pakistan Water and Power Development Authority, Publication, 2014; 299: 155.

[7] Rahim B E A, Yusoff I, Jafri A M, Othman Z, Ghani A A. Application of MIKE SHE modelling system to set up a detailed water balance computation. Water and Environment Journal, 2012; 26(4): 490–503.

[8] Bailey R T, Wible T C, Arabi M, Records R M, Ditty J. Assessing regional-scale spatio-temporal patterns of groundwater-surface water interactions using a coupled SWAT-MODFLOW model. Hydrological Processes, 2016; 30(23): 4420–4433.

[9] Gebreyohannes T, de Smedt F, Walraevens K, Gebresilassie S, Hagos M, Amare K, et al. Application of a spatially distributed water balance model for assessing surface water and groundwater resources in the Geba basin, Tigray, Ethiopia. Journal of Hydrology, 2013; 499: 110–123.

[10] Singh A, Panda S N, Saxena C K, Gupta S K. Optimization modeling for conjunctive use planning of surface water and groundwater for irrigation. Journal of Irrigation and Drainage Engineering, 2015; 142(3): 04015060.

[11] Khan M R, Voss C I, Yu W, Michael H A. Water resources management in the Ganges Basin: a comparison of three strategies for conjunctive use of groundwater and surface water. Water Resources Management, 2014; 28(5): 1235–1250.

[12] Li X L, Yang G, He X L, Zhao C, Wang C, Chen S, et al. Study on Groundwater Level Changes and Water Balance in Manasi River Basin. Journal of China Hydrology, 2016; 36(4): 85–92. (in Chinese)

[13] Li X L, He X L, Yang G, Yang M J. Study on groundwater using visual MODFLOW in the Manas River Basin, China. Water Policy, 2016; 18(5): 1139–1154.

[14] Wang H, Lu C Y, Qin D Y, Sang X F, Li Y, Xiao W H. Advances in method and application of groundwater numerical simulation. Earth Science Frontiers, 2010; 17(6): 1–12. (in Chinese)

[15] Yang X, Liang G H, Zhou H C. Study on Hydrology and Hydrodynamic Model in Guanyinge Shenwo Section of Taizihe River Based on MIKE11. Water Resources and Power, 2010; 28(11): 84–87.

[16] Lin B, Liu Q J, Shang H, Wang Y W, Sui X. Application of coulpled MIKE11/NAM model in Naoli River Basin, northeastern China. Journal of Beijing Forestry University, 2014; 36 (5): 99–108. (in Chinese)

[17] Varouchakis E A, Karatzas G P, Giannopoulos G P. Impact of irrigation scenarios and precipitation projections on the groundwater resources of Viannos Basin at the island of Crete, Greece. Environmental Earth Sciences, 2015; 73(11): 7359–7374.

[18] Darko R O, Yuan S Q, Liu J P, Yan H F, Zhu X Y. Overview of advances in improving uniformity and water use efficiency of sprinkler irrigation. Int J Agric & Biol Eng, 2017; 10(2): 1–15.

[19] Fu Q, Xiao Y Y, Cui S, Liu D, Li T X. Optimization of water use structure and plantation benefit of unit water consumption using fractional programming and conditional value-at-risk model. Int J Agric & Biol Eng, 2017; 10(2): 151–161.